

Chemical Ordering and Boundary Structure in Strained-Layer Si-Ge Superlattices

E. Müller, H.-U. Nissen, M. Ospelt, and H. von Känel

Laboratorium für Festkörperphysik, Eidgenössische Technische Hochschule, Zürich, Switzerland

(Received 14 June 1989)

The interface structure of strained-layer Si-Ge superlattices on Si(100) is investigated by selected-area electron-diffraction techniques and high-resolution transmission electron microscopy. Three types of strained-layer Si-Ge superlattices characterized by different strain distributions are compared. Diffraction evidence is presented for the existence of boundary layers at the interfaces consisting of chemically ordered domains with a bilayer stacking of Si and Ge along the $\langle 111 \rangle$ directions. This phenomenon is independent of the strain distribution between Si and Ge, i.e., of the choice of the substrate lattice parameter.

PACS numbers: 61.16.Di, 61.50.Ks, 68.65.+g

This paper reports on a new phenomenon of ordering of Si and Ge atoms in the boundary layers of strained-layer superlattices (SLS), with layers of pure silicon and germanium on Si(100), found by electron-diffraction techniques. The result is of interest for the currently very active field of band-structure investigations in multilayer systems grown by molecular-beam epitaxy (MBE) and also for diffraction physics and crystallography in general.

The first evidence for new optical transitions in a Si_4Ge_4 strained-layer superlattice on Si(100)^{1,2} has triggered a steadily increasing number of theoretical and experimental investigations exploring the changes of band structure in Si_nGe_m SLS due to strain and zone-folding effects.³⁻¹⁴ While in the theoretical studies sharp interfaces between the individual Si and Ge layers were usually assumed, indications for some degree of interface roughness have been found in all real structures investigated to date.^{1,2,6,12-14} In the present study we have therefore investigated in more detail these deviations from a perfectly periodic structure in Si-Ge SLS on Si(100) grown by MBE. The techniques of selected-area electron diffraction and high-resolution transmission electron microscopy (HRTEM) have been used. Both methods have previously been applied successfully in the investigation of real crystal phenomena in multilayer systems.¹⁵ Three types of SLS characterized by different

strain distributions have been used for the electron microscopic studies; i.e., the SLS were lattice-matched either (1) to Si, (2) to thick relaxed Ge buffers, or (3) to relaxed $\text{Si}_{1-x}\text{Ge}_x$ buffers with an average composition equal to the SLS, resulting in symmetrically strained Si and Ge layers.¹⁶ The samples were grown in a VG V80 MBE system equipped with electron-gun evaporators for Si and an effusion cell for Ge. The growth rates of the SLS were in the range of 0.5–1.0 Å/s. The relevant sample parameters are presented in Table I. The superlattices have been characterized previously by Rutherford backscattering spectroscopy (RBS) and ion-channeling, x-ray diffraction, and Raman scattering.¹⁷ Using these techniques, pseudomorphic growth on the respective buffers has been demonstrated in each of the three cases.

For electron microscopic investigation two different techniques of specimen preparation were used. For taking high-resolution electron micrographs as well as selected-area diffraction patterns, the samples were thinned by ion milling using argon. In order to ensure that the observed diffraction effects were not due to ion-beam damage, the experiments were repeated using specimens cleaved along (110) planes. All diffraction effects reported here have also been observed on the cleaved samples. Since these samples were never exposed to the ion beam, they showed extremely thin amor-

TABLE I. Data for the synthesis of the specimens: T_g , substrate temperature during growth; d , period of the superlattice; d_{Si} , thickness of the Si layers; d_{Ge} , thickness of the Ge layers; χ_{min} , minimum channeling yield.

Specimen number	T_g (°C)	d (Å)	d_{Si} (Å)	d_{Ge} (Å)	Number of periods	Substrate	χ_{min} (%)
232	460	52.8	45.1	7.7	25	Si	3.7
258	470	44.1	39.2	4.9	110	Si	3.4
257	450	12.11	2.95	9.16	80	Ge	6.6
273	400	14.2	8.1	6.1	116	$\text{Si}_{1-x}\text{Ge}_x$	8.7
501	420	13.3	7.7	5.6	380	$\text{Si}_{1-x}\text{Ge}_x$	10
506	420	17.5	8.6	8.9	73	$\text{Si}_{1-x}\text{Ge}_x$	9.9
507/3	420	11.2	9.5	1.7	462	$\text{Si}_{1-x}\text{Ge}_x$	3.1

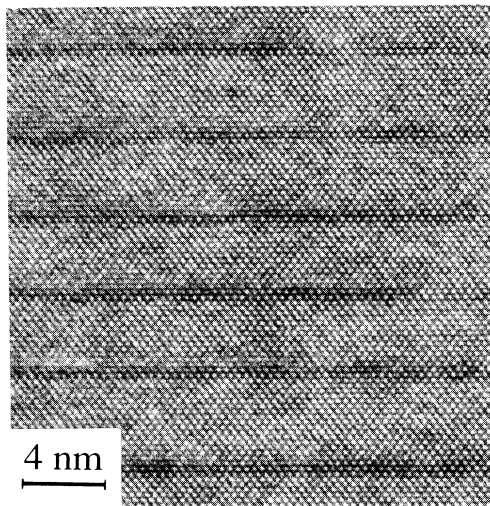


FIG. 1. High-resolution electron micrograph of a strained-layer Si-Ge superlattice on Si(100) in [110] projection (sample 258).

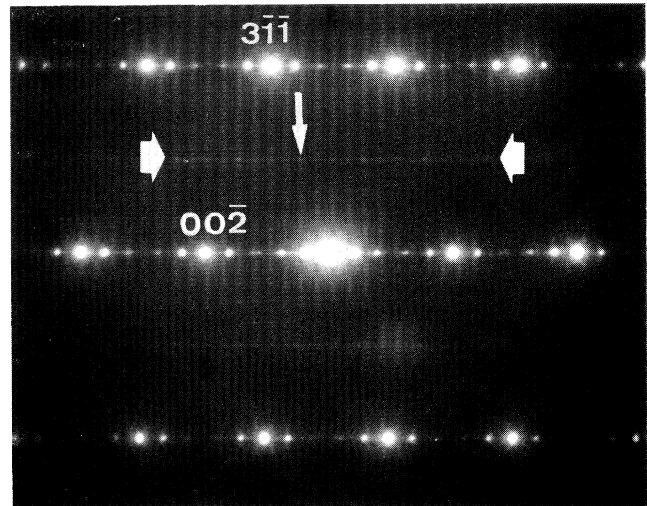


FIG. 2. Diffraction pattern of a short-period superlattice along the [130] axis (specimen 273).

phous surface regions less than 15 Å thick, due to oxidation. These specimens were studied by a 300-kV transmission electron microscope (Phillips CM 30), equipped with a ± 30° tilting goniometer, and a 200-kV instrument (Joel 200 CX) with a ± 10° tilting device.

High-resolution electron micrographs taken along the [110] axis of the three types of multilayer specimens reveal perfect pseudomorphic growth (Fig. 1). Recognizable steps at the interfaces are confined to one atomic monolayer. Selected-area electron-diffraction patterns (Fig. 2) of all types of specimens reveal two noteworthy features: (1) Additional electron-diffraction spots at positions $(h/2, k/2, l/2)$, for h, k, l all odd. (2) Diffuse streaks along the growth direction through all spots of the diamond structure, including the undiffracted beam as well as the half-integer reflections. Note that there is no evidence of an asymmetry with respect to the four equivalent $\langle 111 \rangle$ directions and that apart from variations in the intensity the additional diffraction features have been found in all as-grown specimens, independent of the kind of buffer, the Ge concentration, and the growth temperature. They have also been observed at specimens grown at temperatures below 400 °C.¹⁸

In order to interpret these unusual diffraction phenomena, we assume ordered interfaces with an alternating stacking of two monolayers of each atomic species in one of the four equivalent $\langle 111 \rangle$ directions, i.e., SiSiGeGeSiSiGeGe... [Fig. 3(a)], instead of interfaces characterized by a statistical roughness on a monolayer scale. The model is analogous to similar model structures proposed for the interpretation of diffraction phenomena in strained Si-Ge alloys.^{11,19-22} In order to compare the electron-microscopic contrast of a pure Ge layer with that of a totally ordered structure, the atom posi-

tions shown in Fig. 3(b) were used as a basis for a dynamical multislice calculation.^{23,24} The ordered domain is in the center of the figure. This domain extends over six monolayers along the [001] direction in thickness. The domain is assumed to extend over the entire thickness (24.7 nm) of the specimen. The calculated image (Fig. 4) shows the image contrast for three

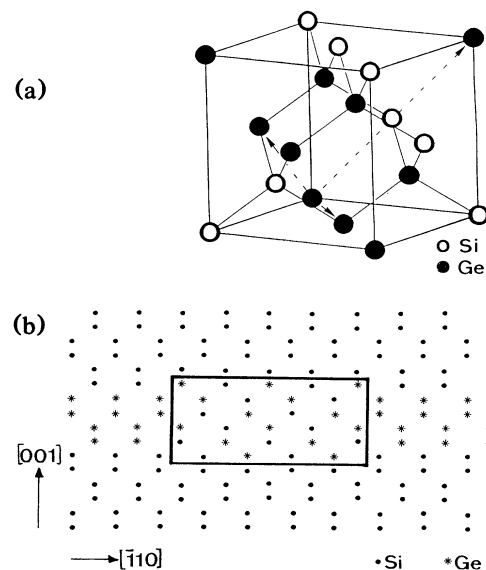


FIG. 3. (a) Diamond-lattice unit cell showing the ordered structure (Ref. 19). (b) [110] projection of the atom positions used for the simulations. The ordered domain (extending six monolayers along the growth direction) is marked by a frame.

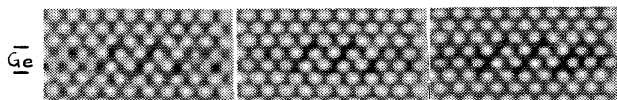


FIG. 4. Image simulation of the ordered structure presented in Fig. 3(b). It shows a specimen 24.7 nm in thickness for three different defocus values, i.e., from left to right, 53, 61, and 69 nm, respectively.

different defocus values, i.e., from left to right, 53, 61, and 69 nm, respectively. Even assuming an extreme case in which the ordered domain extends over the entire thickness of the specimen, the observable modulation of the contrast in the calculated images is very weak, so that electron micrographs can give no information in addition to that obtainable from electron-diffraction results.

The main spots in the electron-diffraction pattern are due to the diamond structure of the Si and the Ge layers, while the additional intensities at half-integer positions originate from the ordered domains. The structure factor can be calculated on the basis of the model for the ordered structure as follows:

$$S = 2 \cos\{2\pi g \cdot (a/8)[111]\} \\ \times \{f_{\text{Si}} + f_{\text{Ge}} \exp(2\pi i g \cdot (a/2)[101])\}.$$

The streaking going through the half-integer reflections is explained by shape effects caused by the chemically ordered domains: In specimens with either Si or Ge layers thicker than approximately four monolayers, the chemically ordered domains are confined to the interfaces; i.e., a mainly two-dimensional ordering effect has to be assumed. Therefore a threadlike intensity distribution along the growth direction can be expected in the selected-area diffraction patterns of these samples. This intensity distribution corresponds to indices $[h, k, l] = [\frac{1}{2}, \frac{1}{2}, \frac{1}{2}] + x[0, 0, 1]$, x real. By contrast, for specimens with either Si or Ge layers thinner than about four monolayers, the ordering may become a three-dimensional phenomenon. Since the domains are ordered along any of the equivalent $\langle 111 \rangle$ directions and only a part of the interfaces will order, there will always be a mixture of two- and three-dimensionally ordered domains. Therefore spots at $[h/2, k/2, l/2]$ for h, k, l all odd are expected as a streaking at $[h, k, l] = [\frac{1}{2}, \frac{1}{2}, \frac{1}{2}] + x[0, 0, 1]$, x real, through these spots. All our observations correspond to these predictions. The local deviations from the average periodicity also contribute to the streaking through the reflections originating from the diamond structure.²⁵

An intriguing feature of our observations is that the observed diffraction phenomena occur in all types of SLS, i.e., independent of the strain distribution in the individual layers. In particular, strain symmetrization apparently does not affect the ordering. This is in agree-

ment with previous studies on thick relaxed $\text{Si}_{1-x}\text{Ge}_x$ alloy layers²⁰ but is not compatible with theoretical calculations requiring asymmetrically strained structures for the ordering phenomenon.^{11,21,22} This causes the question as to the importance of crystalline defects which lead to locally inhomogeneous strains. From Table I it is evident that the crystalline quality in the strain-symmetrized SLS (with the exception of the specimen 507) is inferior to that of the asymmetrically strained structures. However, all other experimental evidence (Raman scattering, x-ray diffraction, and RBS data) indicates that the average strain in the Si and Ge layers of the strain-symmetrized SLS indeed conforms to the predictions of elasticity theory.¹⁷ Besides, the selected-area diffraction patterns taken in the defect-free regions of the strain-symmetrized SLS all show the additional diffraction effects attributed to the ordered domains. Our observations made on specimens grown at temperatures between 400 and 500 °C, as well as those made by a different laboratory on specimens grown at even lower temperatures,¹⁸ indicate that there may be a principal limitation for the perfection of Si-Ge superlattices with ultrashort period. A detailed account of our observations, including Raman measurements, will be given in a subsequent publication.

We acknowledge, with many thanks, fruitful discussions with C. Beeli and the efficient help and instruction of R. Wessicken. We are grateful for financial support by the Swiss National Science Foundation.

¹T. P. Pearsall, J. Bevk, L. C. Feldman, J. M. Bonar, J. P. Mannaerts, and A. Ourmazd, *Phys. Rev. Lett.* **58**, 729 (1987).

²J. Bevk, A. Ourmazd, L. C. Feldman, T. P. Pearsall, J. M. Bonar, B. A. Davidson, and J. P. Mannaerts, *Appl. Phys. Lett.* **50**, 760 (1987).

³S. Froyen, D. M. Wood, and A. Zunger, *Phys. Rev. B* **36**, 4547 (1987).

⁴M. S. Hybertsen and M. Schlüter, *Phys. Rev. B* **36**, 9683 (1987).

⁵L. Brey and C. Tejedor, *Phys. Rev. Lett.* **59**, 1022 (1987).

⁶K. Eberl, G. Krötz, R. Zachai, and G. Abstreiter, *J. Phys. (Paris)* **48**, Suppl. 11, C5-329 (1987).

⁷M. A. Gell, *Phys. Rev. B* **38**, 7535 (1988).

⁸S. Satpathy, R. M. Martins, and C. G. van de Walle, *Phys. Rev. B* **38**, 13237 (1988).

⁹K. B. Wong, M. Jaros, I. Morrison, and J. P. Hagon, *Phys. Rev. Lett.* **60**, 2221 (1988).

¹⁰S. Froyen, D. M. Wood, and A. Zunger, *Phys. Rev. B* **37**, 6893 (1988).

¹¹S. Ciraci and Inder P. Batra, *Phys. Rev. B* **38**, 1835 (1988).

¹²M. S. Hybertsen, M. Schlüter, R. People, S. A. Jackson, D. V. Lang, T. P. Pearsall, J. C. Bean, J. M. Vandenberg, and J. Bevk, *Phys. Rev. B* **37**, 10195 (1988).

¹³G. Abstreiter, K. Eberl, E. Friess, W. Wegscheider, and R. Zachai, *J. Cryst. Growth* **95**, 431 (1989).

¹⁴T. P. Pearsall, J. Bevk, J. C. Bean, J. Bonar, J. P. Man-
naerts, and A. Ourmazd, *Phys. Rev. B* **39**, 3741 (1989).

¹⁵T. S. Kuan, T. F. Kuech, W. I. Wang, and E. L. Wilkie,
Phys. Rev. Lett. **54**, 201 (1985).

¹⁶E. Kasper, H.-J. Herzog, H. Jorke, and G. Abstreiter, *Superlattices Microstruct.* **3**, 141 (1987).

¹⁷M. Ospelt, W. Bacsa, J. Henz, K. A. Mäder, and H. von
Känel, *Superlattices Microstruct.* **5**, 71 (1989).

¹⁸K. Eberl and E. Friess, Walter Schottky Institut, Tech-
nische Universität München (private communication).

¹⁹A. Ourmazd and J. C. Bean, *Phys. Rev. Lett.* **55**, 765
(1985).

²⁰D. J. Lockwood, K. Rajan, E. W. Fenton, J.-M. Baribeau,
and M. W. Denhoff, *Solid State Commun.* **61**, 465 (1987).

²¹P. B. Littlewood, *Phys. Rev. B* **34**, 1363 (1986).

²²J. L. Martins and A. Zunger, *Phys. Rev. Lett.* **56**, 1400
(1986).

²³P. A. Stadelmann, *Ultramicroscopy* **21**, 131 (1987).

²⁴E. Müller, H.-U. Nissen, M. Ospelt, H. von Känel, and P.
Stadelmann, in *Proceedings of the European Materials
Research Society, Third International Symposium on Si
Molecular-Beam Epitaxy, Strasbourg, France, 1989* (to be
published).

²⁵W. Bollmann, *Z. Kristallogr.* **126**, 1 (1968).

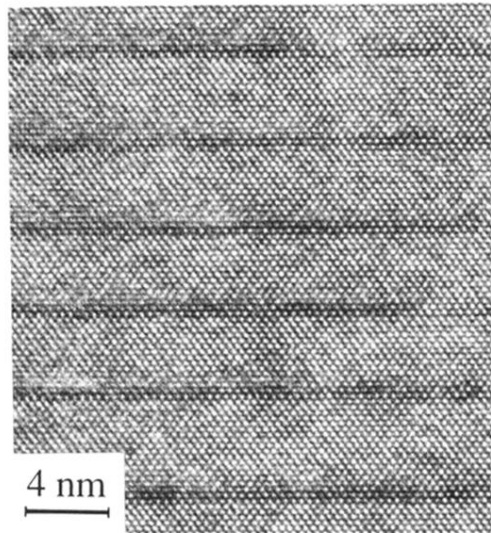


FIG. 1. High-resolution electron micrograph of a strained-layer Si-Ge superlattice on Si(100) in [110] projection (sample 258).

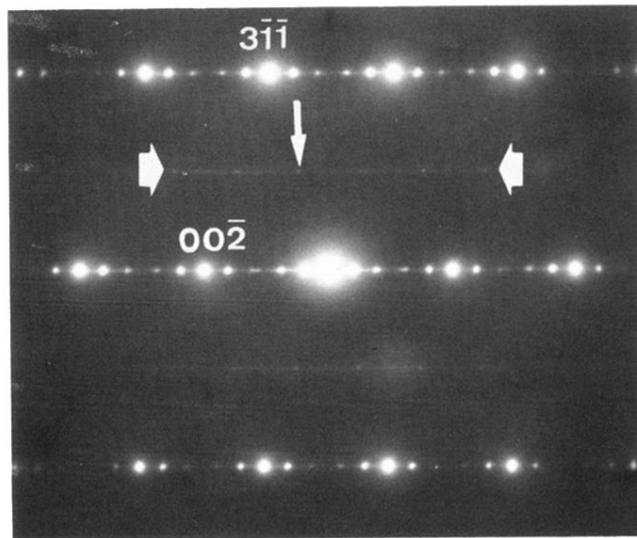


FIG. 2. Diffraction pattern of a short-period superlattice along the $[130]$ axis (specimen 273).

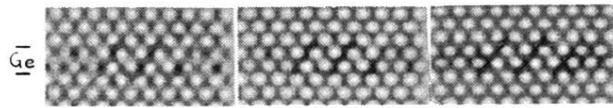


FIG. 4. Image simulation of the ordered structure presented in Fig. 3(b). It shows a specimen 24.7 nm in thickness for three different defocus values, i.e., from left to right, 53, 61, and 69 nm, respectively.